NANO LETTERS

2008
Vol. 8, No. 11
3776-3780

Nanowire Conductive Polymer Gas Sensor Patterned Using Self-Assembled Block Copolymer Lithography

Yeon Sik Jung,[†] WooChul Jung,[†] Harry L. Tuller, and C. A. Ross*

Department of Materials Science and Engineering, Massachusetts Institute of Technology, Cambridge, Massachusetts 02139

Received July 15, 2008; Revised Manuscript Received September 17, 2008

ABSTRACT

Nanostructured conjugated organic thin films are essential building blocks for highly integrated organic devices. We demonstrate the large-area fabrication of an array of well-ordered 15 nm wide conducting polymer nanowires by using an etch mask consisting of self-assembled patterns of cylinder-forming poly(styrene-b-dimethylsiloxane) diblock copolymer confined in topographic templates. The poly(3,4-ethylenedioxythiophene):poly(styrenesulfonate) nanowires operated as an ethanol vapor sensor, suggesting that the electronic properties of the organic film were preserved during the patterning processes. The higher sensitivity to ethanol vapor, compared to an unpatterned film with the same thickness, was attributed to the enhanced surface-to-volume ratio of the nanowire array.

A molecular rectifier, theoretically proposed by Ratner and Aviram in 1974, was the starting point for a boom in molecular electronics research that has persisted for the last three decades.[1] Later, single-molecule field-effect transistors and logic gates were also conceptually proposed,[2] and Reed et al. first reported single-molecule conductance measurements through benzene-1,4-dithiol.[3] The development of conductive polymers has continued to attract interest for many different applications including optoelectronic devices,[4−6] field effect transistors,[7,8] and chemical or biological sensors.[8,9] In these applications, device performance has been improved by miniaturizing the feature sizes down to the nanoscale regime,[10,11] and there is considerable interest in methods that enable the patterning of electronically active polymers on the nanoscale.

Various fabrication techniques have been developed for generating conducting polymer nanowires. Chemical or electrochemical growth without templates usually produces entangled nanowires with a large distribution in diameter and length, which is undesirable in terms of performance and reproducibility, despite the convenience of fabrication.[12−17] For better-organized structures, scanning-probe and electron-beam patterning have been employed to direct the growth of conducting polymer nanowires.[11,18,19] Recently, spontaneous ordering of polymer nanowires was induced within a submicron gap between electrodes fabricated using a focused ion beam.[20] However, the throughput and manufacturability of these methods are limited by the serial nature of the patterning techniques. Well-ordered conducting polymer nanopatterns have also been produced by nanoimprint lithography,[21] but this technique requires fabrication of master molds.

In this communication, we report fabrication of well-ordered arrays of 15 nm wide, 35 nm period poly(3,4-ethylenedioxythiophene):poly(styrenesulfonate) (PEDOT:PSS) conducting polymer nanowires, made over areas of several square centimeters using a self-assembled block copolymer mask, and we demonstrate the capability of the patterned structures to act as an ethanol vapor sensor, confirming the preservation of the electronic properties of the PEDOT:PSS during patterning. Block copolymer self-assembly is a simple, cost-effective, and scalable maskless nanofabrication technique, in which the feature sizes and geometries can be controlled via the chain length and volume fractions of the blocks.[22−24] Previously, we have described the self-assembly of a poly(styrene-b-dimethylsiloxane) (PS-PDMS) diblock copolymer, which forms extraordinarily well-ordered structures due to its large Flory−Huggins interaction parameter.[25−27] The structures have an excellent etch-selectivity between the two polymer blocks as a result of the high Si content in the PDMS block,[25−27] and this facilitates pattern transfer into an underlying functional material. PEDOT:PSS was chosen for this study due to its superior stability and conductivity compared to other conducting polymers such as polypyrrole.[28] The well-organized conductive polymer nanowire arrays formed by this method may be useful for nanoscale

* To whom correspondence should be addressed. Email: caross@mit.edu. Tel.: 617-258-0223. Fax: 617-252-1020.
[†] These authors contributed equally to this work.

10.1021/nl802099k CCC: $40.75 © 2008 American Chemical Society
Published on Web 10/28/2008

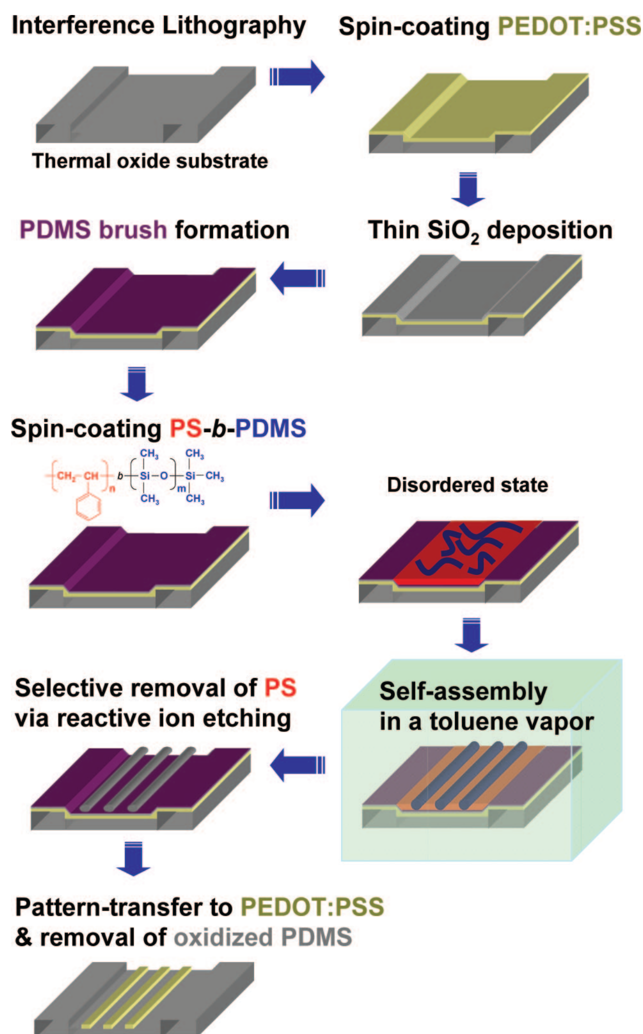

Figure 1. Procedure for polymer nanowire fabrication. An aqueous PEDOT:PSS solution was spin-coated on a substrate patterned with a 1.3 μm period grating, then coated with a thin SiO_2 layer and a PDMS homopolymer brush. A PS-PDMS block copolymer thin film was then spin-coated and solvent-annealed. The self-assembled block copolymer patterns were transferred into the underlying PEDOT:PSS film through a series of reactive ion etching steps employing CF_4 and O_2 plasmas.

organic device components such as interconnect lines or electrodes.

The procedure to fabricate PEDOT:PSS nanowires is depicted in Figure 1 and described in detail in the Methods section. The fabrication process is based on self-assembly of a PS-PDMS block copolymer film on a substrate. The silica-coated silicon substrate was initially patterned with 40 nm deep, 1.3 μm period trenches and then coated with PEDOT:PSS (20 nm), SiO_2 (5 nm) and a thin (3−4 nm) PDMS homopolymer brush. The silica layer provides a surface for grafting of the homopolymer, which improves the quality of the self-assembled PS-PDMS pattern.[25] The PS-PDMS block copolymer was spin-coated on this multilayer substrate and solvent annealed, leading to arrays of parallel PDMS cylinders in a PS matrix within the trenches. The arrays of PDMS cylinders, with thickness of 12 - 13 nm, period 35 nm, and width 15 nm, was etched into the underlying PEDOT:PSS film to form nanowires of PEDOT:

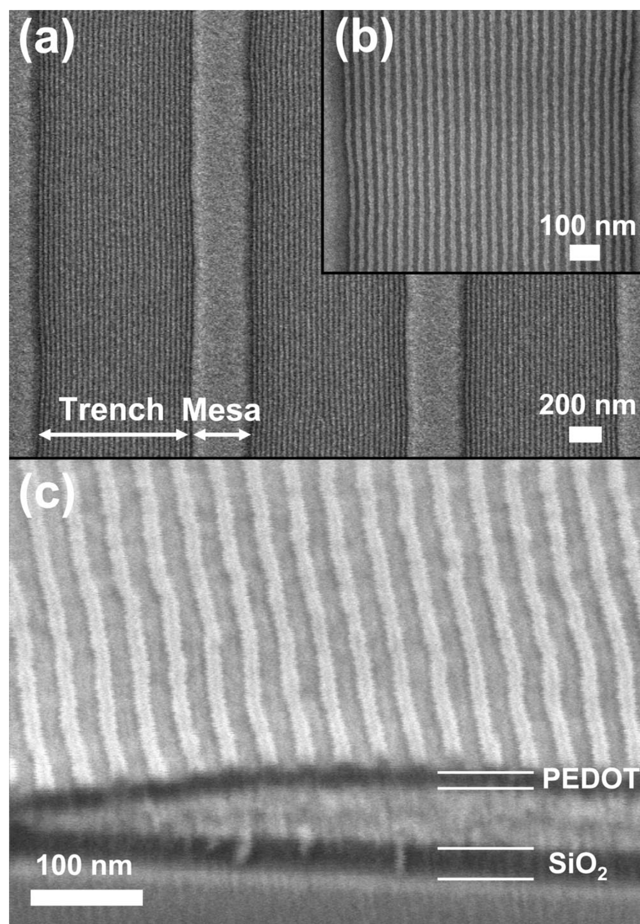

Figure 2. Self-assembled block copolymer patterns after two-step reactive ion etching composed of a 5 s, 50 W, CF_4 etch followed by a 30 s 90 W, O_2 etch.

PSS. As shown in Figure 2, the self-assembled PS-PDMS block copolymer patterns show an excellent degree of ordering within the trenches, with quality similar to that obtained previously in trenches etched into silicon and coated with a thin PDMS brush.[25] Although the cylinders adjacent to the trench edges show some edge roughness, correlated to roughness in the trench walls, the cylinders closer to the center of the groove are very straight with an edge roughness of 3.6 nm.

Self-assembled block copolymer patterns have been transferred into a range of metallic, oxide, and semiconductor materials,[25,29−31] but pattern transfer into functional polymers is more challenging. First, the underlying functional polymer must have a very low surface roughness, so that self-assembly of the block copolymer is not kinetically hindered. Second, the underlying polymer must be tolerant to the processing conditions used to form the homopolymer brush layer, or to promote microphase segregation in the block copolymer. In this case, the brush layer formation is carried out at 170 °C for over 10 h, while the solvent annealing of the block copolymer is carried out in toluene vapor for 17 h. This requirement precludes the patterning of polymers with a low glass transition temperature, which may agglomerate on heating, or polymers soluble in toluene, for example, polystyrene or polymethylmethacrylate, which can swell by

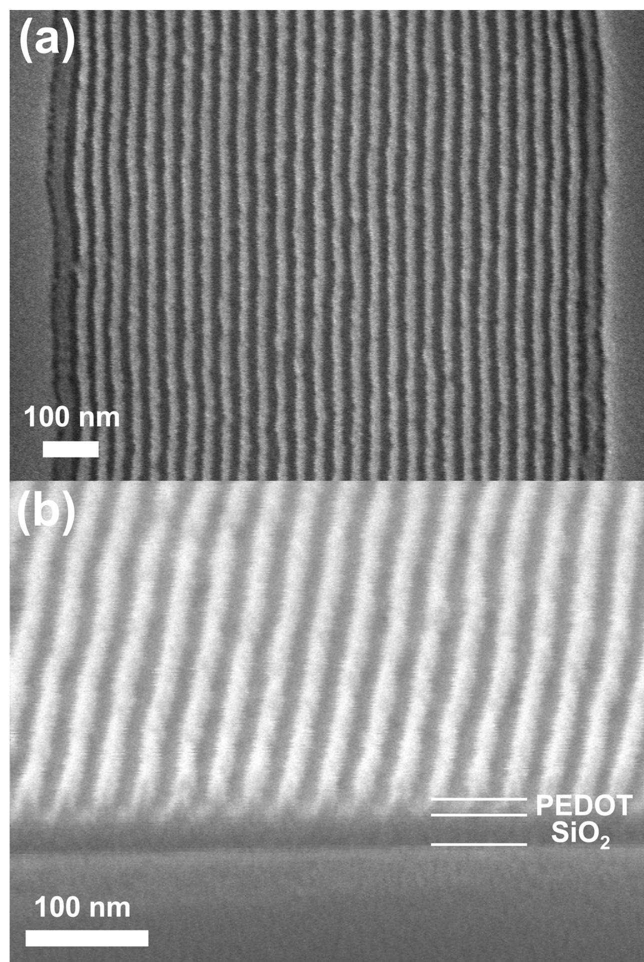

Figure 3. PEDOT:PSS nanowires after 30 s, 50 W, O_2/He reactive ion etching, using the self-assembled PDMS patterns as an etch mask. The remaining PDMS and thin oxide interlayer were removed with an additional CF_4 plasma treatment.

toluene vapor uptake. However, spin-coated PEDOT:PSS films satisfy these criteria since they are smooth (root-mean-square roughness <0.8 nm), thermally stable at 170 °C, and poorly soluble in toluene.

Patterned conducting polymer nanowires with a width of 15 nm and a height of 20 nm are shown in Figure 3. On a 1.7 × 1.7 cm^2 substrate, around 3.8 × 10^5 parallel conducting polymer nanowires were produced. To our knowledge, these PEDOT:PSS nanowires have the highest pattern density reported for conducting polymer nanowires. This patterning method therefore represents a simple and manufacturable process that is capable of defining large areas of nanoscale features in soft materials with a high aspect ratio (height/width), which is 1.33 in this case. The line edge roughness of the PEDOT:PSS patterns was 5.7 nm, larger than the 3.6 nm edge roughness of the block copolymer patterns.

To test whether patterning affected the electrical properties of the polymer, we fabricated a two-terminal chemiresistor gas sensor device based on the reversible change in electrical conductivity of the polymer as it swells upon exposure to an organic vapor.[32,33] Uptake of small organic molecules changes the chain conformation and affects charge carrier hopping between the chains. The degree of swelling depends on the partial vapor pressure and the interaction between the polymer and organic vapor. Figure 4a schematically illustrates the formation of Au electrodes on top of the polymer nanopattern, enabling a large number (1.3 × 10^5) of nanowires to be measured in parallel. The linear current−voltage curve, as seen in the inset of Figure 4b, indicates that an ohmic contact was formed between the electrodes and the PEDOT:PSS. Figure 4b shows the response of the conducting polymer nanowires to varying ethanol concentrations in the nitrogen carrier gas. The response, $\Delta R/R_0$, increased with the partial pressure of ethanol in the gas phase, confirming

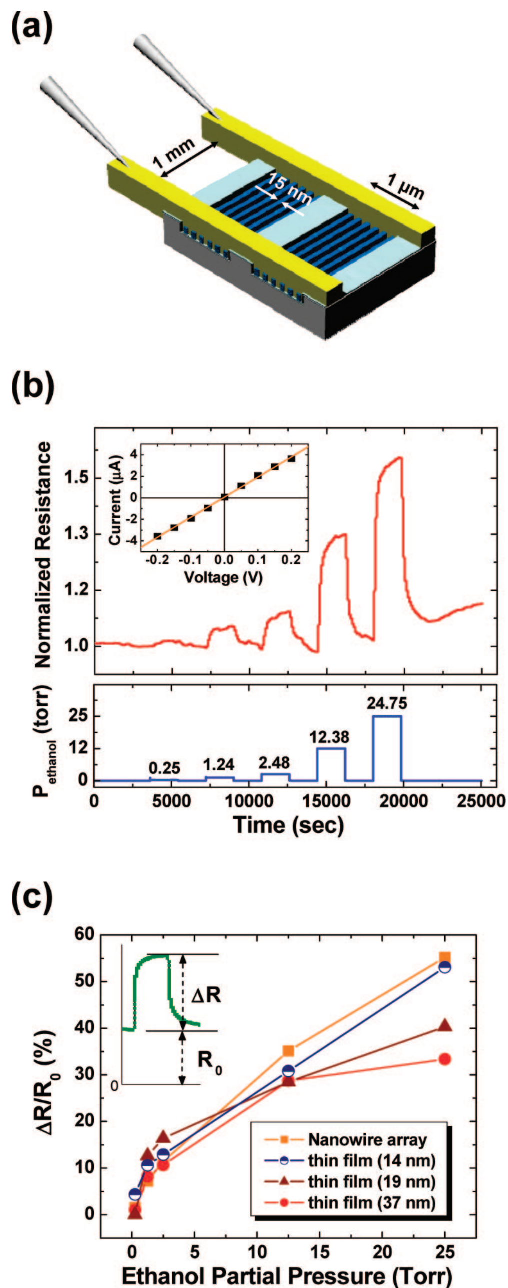

Figure 4. (a) Schematic (not to scale) of a chemiresistor for ethanol vapor detector based on PEDOT:PSS nanowires. Fifty nanometer thick Au electrodes, 1 mm apart, are formed perpendicular to the nanowires. (b) The resistance change of the polymer nanowires upon exposure to ethanol vapor. (c) Comparison of the response ($\Delta R/R_o$) of the nanowire array with that of thin films of three different thicknesses (14, 19, and 37 nm).

the ability of the nanowires to operate as an ethanol vapor detector, despite any damage to the PEDOT:PSS originating from the RIE processes. The resistance changes are observed to be largely reversible with some upward drift in R_0 apparent at larger partial pressures of ethanol. On the basis of the assumption that the ethanol vapor from the bubbler is fully saturated, the concentration of ethanol vapor was calculated from the equilibrium vapor pressure of ethanol (49.5 Torr at 22 °C), and thereby an ethanol detection limit may be estimated. Even the smallest partial pressure (0.25 Torr) of ethanol vapor, corresponding to 325 ppm, exhibits a relative resistance change of 1.5% as shown in Figure 4c. Both the polymer nanowires and thin films show a partial irreversibility of resistance as high as 3−5% especially for a large concentration of ethanol, which is consistent with previous reports.[34,35] This is attributed to a nonequilibrium configuration of the chains in the as-deposited material, which rearrange in the presence of ethanol vapor, giving an aging effect.

The response $\Delta R/R_0$ of the nanowire array is compared with that of three thin films in Figure 4c. All of the samples show an increase in $\Delta R/R_0$ with increased partial pressure of ethanol vapor. There is an evident divergence in response between the different thicknesses at the highest vapor pressure of 24.75 Torr, and so we examine the influence of geometry here more carefully. At this pressure, the nanowires (20 nm thick, 15 nm wide) show a considerably higher $\Delta R/R_0$ response compared to the 19 and 37 nm thick films, but similar to that of the 14 nm thick film. This appears to be due to the thicker films exhibiting a saturation in response to higher ethanol vapor pressure. This result is consistent with a previous report on polyaniline, which showed that as film thickness decreases, the sensitivity increases and that if the film is thin enough, a sensitivity close to that of a nanostructured material can be obtained.[33]

It has been suggested that a higher surface-to-volume ratio causes faster diffusion of solvent molecules, and this gives nanostructured materials and thinner films a faster, higher amplitude response.[13,15,20,21,33,35] In inorganic materials used for vapor detection, gas adsorption on the surface induces a Fermi level shift and carrier depletion near the surface, which explains the enhanced sensitivity for devices with higher surface area.[36] However, swelling of a polymer, which is responsible for the electrical response of the PEDOT:PSS to ethanol vapor, occurs throughout its volume, and thus a higher diffusion rate, while leading to a faster response, should not lead to higher sensitivity at equilibrium. That is, unless we assume that the near-surface region has a higher equilibrium solubility for a given vapor pressure compared to the bulk, due to a larger free energy resulting from added surface energy and smaller conformational entropy.[37,38] While this would explain the trends in Figure 4c for the highest gas concentrations, it does not explain the near equal responses of all the devices to ethanol partial pressures of 2.5 Torr and below. It is more likely that the difference in sensitivity between the samples is caused by a kinetic limitation related to the longer characteristic diffusion lengths associated with the thicker structures. Particularly for high vapor pressures, considerable residual swelling remains in the thicker films from previous exposures, leading to an apparent decrease in sensitivity for these films.

This work has demonstrated the fabrication of a nanowire ethanol vapor sensor from a film of PEDOT:PSS conducting polymer, patterned into a nanowire array using a block copolymer self-assembled within a topographical template. The nanowire array shows a higher and more linear resistance response than an unpatterned film with the same thickness, which is attributed to its high surface area to volume ratio and to its short diffusion length. The fact that the conducting properties of the film are preserved through the etching process further suggests that self-assembled nanolithography may also be applied to fabricate other conductive conjugated polymers to form active devices such as light-emitting diodes, memories, or transistor arrays.

Methods. ***Nanowire Fabrication.*** The substrates used were Si wafers with 30 nm thick thermal oxide layers coated with a 40 nm thick layer of sputtered silica. The substrates were patterned over areas of 1.7 × 1.7 cm^2 with parallel trenches with period of approximately 1.3 μm, width 1 μm and depth 40 nm. The trenches were made by coating the substrates with a positive resist (PFI-88) and exposing them with a grating pattern using a Lloyd's Mirror interference lithography system with a 325 nm wavelength He−Cd laser. Reactive ion etching (RIE) with a CF_4 plasma was used to transfer the grating pattern into the deposited silica. Twenty nanometer thick PEDOT:PSS thin films were spin-coated on the grating patterns from a 1.3 wt % aqueous solution of PEDOT:PSS purchased from Sigma-Aldrich and diluted to 0.87 wt % with deionized water. To remove agglomerated particles, the solution was filtered through a 0.25 μm membrane (Nalgene) before use. After spin-coating, the films were dried at 150 °C for two minutes to remove moisture. Then, a thin silica film (5 nm) was sputter-deposited, and the silica surface was modified by hydroxy-terminated PDMS homopolymer with a molecular weight 5 kg/mol, which was spin-cast on the substrates and annealed at 170 °C for 15 h, then washed with toluene to remove unreacted polymer. The thickness of the grafted brush layer was estimated to be 3−4 nm by ellipsometry. The diblock copolymer of PS-PDMS with overall molecular weight of 45.5 kg/mol and volume fraction of PDMS of 33.5% was purchased from Polymer Source, Inc. To obtain 35 nm thick thin films, toluene solutions of 1.5% by weight of the block copolymer were spin-coated onto the substrates. Solvent-annealing in toluene vapor promoted self-assembly of the block copolymer into a structure consisting of in-plane cylinders of PDMS within a PS matrix, with a PDMS layer at the surface and at the substrate interface. Reactive ion etching was used to remove the PDMS surface layer (with a CF_4 plasma) and the PS matrix (with an O_2 plasma), leaving well-ordered arrays of oxidized PDMS cylinders.[25] These patterns were then transferred into the PEDOT:PSS layer using further reactive ion etch steps. To begin with, the very thin oxidized PDMS brush layer and the 5 nm thick SiO_2 film were etched with a short CF_4 plasma, leading to a structure consisting of 12−13 nm thick oxidized PDMS cylinders on top of the

PEDOT:PSS layer. The PEDOT:PSS layer was then etched with an O_2 plasma to form in-plane nanowires of PEDOT:PSS. A controlled overetching process using the 30 nm thick underlying SiO_2 as an etch stopper was employed to ensure a complete removal of the polymer film in unmasked areas. The etch selectivity between PEDOT:PSS and the oxidized PDMS mask is at least 10:1. The remaining oxidized PDMS was removed with another CF_4 plasma treatment step.

Electrical Testing. The sensitivity of PEDOT:PSS nanowires and films to ethanol vapor was tested at room temperature. Au electrodes were deposited on top of the film or nanowire arrays by DC sputtering with a power of 50 W and an Ar working pressure of 10 mTorr. Two rectangular 1 mm × 6 mm Au electrodes with a 1 mm interelectrode gap were fabricated using a stainless steel shadow mask. The samples were mounted on Al_2O_3 sample holders and contacted by Pt wires that were attached to the sputtered Au electrodes using silver paste (SPI Silver Paste Plus, SPI Supplies, Chester, PA, USA). The sample holders were then inserted inside a quartz tube chamber (16 mm inner diameter, 300 mm length, G. Finkenbeiner Inc., Waltham, MA) to which inlet and outlet fittings had been attached. Mass flow controllers (MKS 1359C mass flow controllers and an MKS 647A controller unit) regulated the flow of nitrogen (99.998% purity) carrier gas through the two lines. One line was bubbled through liquid ethanol, providing a known flow rate of a saturated vapor. To eliminate interference effects due to changes in gas flow rate, the tests were carried out at a constant flow rate of total 200 sccm by mixing the ethanol/nitrogen gas with pure nitrogen from a second line. Thus, the ethanol concentration was varied from 0.5 to 50% of the saturated vapor. The resistance was measured under a DC bias voltage between 0.01 and 0.1 V using a DC power supply and picoammeter (HP 6626A and 4349B, respectively). R_0 is defined as the reference resistance measured in pure nitrogen while ΔR is the resistance change induced by exposure to ethanol in nitrogen. The relative sensitivity to ethanol is then given in terms of $\Delta R/R_0$. The current−voltage response (HP 4142B Modular DC Source/Monitor) showed that this voltage lies within the linear regime of the sample's current−voltage response.

Acknowledgment. C.A.R. and Y.S.J. acknowledge financial support from the Semiconductor Research Corporation. W.C.J. thanks the Samsung Scholarship and H.L.T. thanks the DARPA/HP Focus Center on Non-Lithographic Techniques for MEMS/NEMS at MIT for their financial support.

References

(1) Aviram, A.; Ratner, M. A. *Chem. Phys. Lett.* **1974**, *29* (2), 277–283.
(2) Aviram, A. *J. Am. Chem. Soc.* **1988**, *110* (17), 5687–5692.
(3) Reed, M. A.; Zhou, C.; Muller, C. J.; Burgin, T. P.; Tour, J. M. *Science* **1997**, *278* (5336), 252–254.
(4) Braun, D.; Heeger, A. J. *Appl. Phys. Lett.* **1991**, *58* (18), 1982–1984.
(5) Pei, Q. B.; Yu, G.; Zhang, C.; Yang, Y.; Heeger, A. J. *Science* **1995**, *269* (5227), 1086–1088.
(6) Sirringhaus, H.; Tessler, N.; Friend, R. H. *Science* **1998**, *280* (5370), 1741–1744.
(7) Sirringhaus, H.; Brown, P. J.; Friend, R. H.; Nielsen, M. M.; Bechgaard, K.; Langeveld-Voss, B. M. W.; Spiering, A. J. H.; Janssen, R. A. J.; Meijer, E. W.; Herwig, P.; de Leeuw, D. M. *Nature* **1999**, *401* (6754), 685–688.
(8) Garnier, F.; Hajlaoui, R.; Yassar, A.; Srivastava, P. *Science* **1994**, *265* (5179), 1684–1686.
(9) Gaylord, B. S.; Heeger, A. J.; Bazan, G. C. *J. Am. Chem. Soc.* **2003**, *125* (4), 896–900.
(10) Zhang, J.; Wang, B. J.; Ju, X.; Liu, T.; Hu, T. D. *Polymer* **2001**, *42* (8), 3697–3702.
(11) Liu, H. Q.; Kameoka, J.; Czaplewski, D. A.; Craighead, H. G. *Nano Lett.* **2004**, *4* (4), 671–675.
(12) He, H. X.; Li, C. Z.; Tao, N. J. *Appl. Phys. Lett.* **2001**, *78* (6), 811–813.
(13) Huang, J. X.; Virji, S.; Weiller, B. H.; Kaner, R. B. *J. Am. Chem. Soc.* **2003**, *125* (2), 314–315.
(14) Forzani, E. S.; Zhang, H. Q.; Nagahara, L. A.; Amlani, I.; Tsui, R.; Tao, N. J. *Nano Lett.* **2004**, *4* (9), 1785–1788.
(15) Huang, J. X.; Kaner, R. B. *J. Am. Chem. Soc.* **2004**, *126* (3), 851–855.
(16) Alam, M. M.; Wang, J.; Guo, Y. Y.; Lee, S. P.; Tseng, H. R. *J. Phys. Chem. B* **2005**, *109* (26), 12777–12784.
(17) Wang, Y. J.; Coti, K. K.; Jun, W.; Alam, M. M.; Shyue, J. J.; Lu, W. X.; Padture, N. P.; Tseng, H. R. *Nanotechnology* **2007**, *18* (42), 424021.
(18) Yun, M. H.; Myung, N. V.; Vasquez, R. P.; Lee, C. S.; Menke, E.; Penner, R. M. *Nano Lett.* **2004**, *4* (3), 419–422.
(19) Ramanathan, K.; Bangar, M. A.; Yun, M. H.; Chen, W. F.; Mulchandani, A.; Myung, N. V. *Nano Lett.* **2004**, *4* (7), 1237–1239.
(20) Kemp, N. T.; McGrouther, D.; Cochrane, J. W.; Newbury, R. *Adv. Mater.* **2007**, *19* (18), 2634–2638.
(21) Dong, B.; Lu, N.; Zelsmann, M.; Kehagias, N.; Fuchs, H.; Torres, C. M. S.; Chi, L. F. *Adv. Funct. Mater.* **2006**, *16* (15), 1937–1942.
(22) Park, M.; Harrison, C.; Chaikin, P. M.; Register, R. A.; Adamson, D. H. *Science* **1997**, *276* (5317), 1401–1404.
(23) Schaffer, E.; Thurn-Albrecht, T.; Russell, T. P.; Steiner, U. *Nature* **2000**, *403* (6772), 874–877.
(24) Cheng, J. Y.; Ross, C. A.; Smith, H. I.; Thomas, E. L. *Adv. Mater.* **2006**, *18* (19), 2505–2521.
(25) Jung, Y. S.; Ross, C. A. *Nano Lett.* **2007**, *7* (7), 2046–2050.
(26) Bita, I.; Yang, J. K. W.; Jung, Y. S.; Ross, C. A.; Thomas, E. L.; Berggren, K. K. *Science* **2008**, *321* (5891), 939–943.
(27) Jung, Y. S.; Jung, W.; Ross, C. A. *Nano Lett.* **2008**, *8* (9), 2975−2981.
(28) Sotzing, G. A.; Briglin, S. M.; Grubbs, R. H.; Lewis, N. S. *Anal. Chem.* **2000**, *72* (14), 3181–3190.
(29) Cheng, J. Y.; Ross, C. A.; Chan, V. Z. H.; Thomas, E. L.; Lammertink, R. G. H.; Vancso, G. J. *Adv. Mater.* **2001**, *13* (15), 1174–1178.
(30) Black, C. T. *Appl. Phys. Lett.* **2005**, *87* (16), 163116.
(31) Chai, J.; Wang, D.; Fan, X. N.; Buriak, J. M. *Nat. Nanotechnol.* **2007**, *2* (8), 500–506.
(32) Albert, K. J.; Lewis, N. S.; Schauer, C. L.; Sotzing, G. A.; Stitzel, S. E.; Vaid, T. P.; Walt, D. R. *Chem. Rev.* **2000**, *100* (7), 2595–2626.
(33) Virji, S.; Huang, J. X.; Kaner, R. B.; Weiller, B. H. *Nano Lett.* **2004**, *4* (3), 491–496.
(34) Mabrook, M. F.; Pearson, C.; Petty, M. C. *Appl. Phys. Lett.* **2005**, *86* (1), 013507.
(35) Dan, Y. P.; Cao, Y. Y.; Mallouk, T. E.; Johnson, A. T.; Evoy, S. *Sens. Actuators, B* **2007**, *125* (1), 55–59.
(36) Kolmakov, A.; Moskovits, M. *Annu. Rev. Mater. Res.* **2004**, *34*, 151–180.
(37) Wattenbarger, M. R.; Chan, H. S.; Evans, D. F.; Bloomfield, V. A.; Dill, K. A. *J. Chem. Phys.* **1990**, *93* (11), 8343–8351.
(38) Khayet, M.; Alvarez, M. V.; Khulbe, K. C.; Matsuura, T. *Surf. Sci.* **2007**, *601* (4), 885–895.

NL802099K